nature geoscience

SUPPLEMENTARY INFORMATION

https://doi.org/10.1038/s41561-018-0286-2

In the format provided by the authors and unedited.

Disproportionately strong climate forcing from extratropical explosive volcanic eruptions

Matthew Toohey[1]*, Kirstin Krüger[2], Hauke Schmidt[3], Claudia Timmreck[3], Michael Sigl[2,4,5], Markus Stoffel[6,7,8] and Rob Wilson[9,10]

[1]GEOMAR Helmholtz Centre for Ocean Research Kiel, Kiel, Germany. [2]Department of Geosciences, University of Oslo, Oslo, Norway. [3]Max Planck Institute for Meteorology, Hamburg, Germany. [4]Laboratory of Environmental Chemistry, Paul Scherrer Institute, Villigen, Switzerland. [5]Oeschger Centre for Climate Change Research, Bern, Switzerland. [6]Climate Change Impacts and Risks in the Anthropocene (C-CIA), Institute for Environmental Sciences, University of Geneva, Geneva, Switzerland. [7]dendrolab.ch, Department of Earth Sciences, University of Geneva, Geneva, Switzerland. [8]Department F.-A. Forel for Aquatic and Environmental Sciences, University of Geneva, Geneva, Switzerland. [9]School of Earth and Environmental Sciences, University of St Andrews, Fife, UK. [10]Lamont-Doherty Earth Observatory, Columbia University, Palisades, NY, USA. *e-mail: mtoohey@geomar.de

Supplementary Information for:
Disproportionately strong climate forcing from explosive extratropical volcanic eruptions

Matthew Toohey*[,1], Kirstin Krüger[2], Hauke Schmidt[3], Claudia Timmreck[3], Michael Sigl[2,4,5], Markus Stoffel[6,7,8], Rob Wilson[9,10]

[1]GEOMAR Helmholtz Centre for Ocean Research Kiel, Germany

[2]University of Oslo, Department of Geosciences, Oslo, Norway

[3]Max Planck Institute for Meteorology, Hamburg, Germany

[4]Laboratory of Environmental Chemistry, Paul Scherrer Institute, 5232 Villigen, Switzerland

[5]Oeschger Centre for Climate Change Research, 3012 Bern, Switzerland

[6]Climate Change Impacts and Risks in the Anthropocene (C-CIA), Institute for Environmental Sciences, University of Geneva, Boulevard Carl-Vogt 66, CH-1205 Geneva, Switzerland

[7]dendrolab.ch, Department of Earth Sciences, University of Geneva, Rue des Maraîchers 13, CH-1205 Geneva, Switzerland

[8]Department F.-A. Forel for Aquatic and Environmental Sciences, University of Geneva, Boulevard Carl-Vogt 66, CH-1205 Geneva, Switzerland

[9]School of Earth and Environmental Sciences, University of St Andrews, Fife KY16 9AL, UK

[10]Lamont-Doherty Earth Observatory, Columbia University, Palisades NY 10964, USA

*Corresponding author: mtoohey@geomar.de

Supplementary Table 1: Eruptions excluded from analysis due to potential impact of prior eruptions on NH temperature.

Eruption year	VSSI (Tg S)	Region (1=tropical, 2=NH)	Interfering eruption year
1457	33.0	1	1452
1815	28.1	1	1808
1600	18.9	1	1595
1694	15.7	1	1692
1285	15.1	1	1275
1835	9.5	1	1831
1190	8.5	1	1182
1673	4.7	1	1667
858	4.0	1	853
822	3.9	2	817
904	3.9	2	899
1967	3.4	1	1963
756	3.1	2	750
1692	2.8	1	1694
1766	2.5	2	1761
1646	2.4	2	1640
1822	2.0	1	1815

Supplementary Table 2: Extratropical eruption events excluded from the analysis due to linking of Greenland volcanic sulfate signal to an Icelandic eruption of partially or fully effusive character. Listed with the excluded events are volcanic stratospheric sulfur injection (VSSI) estimates[1] and associated post-eruption 3-year mean temperature anomalies from the mean of all N-TREND[2], STO15[3] and SCH15[4] tree ring-based NH temperature reconstructions.

eVolv2k eruption year(s)	Eruption start date	Volcano (eruption)	VSSI (Tg S)	ΔT_{3yr}^{ALL} (°C)	$\Delta T_{3yr}^{ALL}/VSSI$ (°C [Tg S]$^{-1}$)
1783	June 8, 1783[5]	Grímsvötn (Lakagígar aka "Laki")	20.8	-0.49	-0.024
1477	1477[5]	Bárðarbunga (Veiðivötn)	5.1	-0.29	-0.018
939	Spring 939[6]	Katla (Eldgjá)	16.2	-0.10	-0.011
876, 879, 880	877 ± 1[7]	Bárðarbunga (Vatnaöldur aka Landnám)	6.25[a]	0.07	0.015
822	822[8]	Katla	3.9	NA[b]	NA[b]
817	Unknown	Possibly Katla[8]	9.3[c]	-0.02	-0.006

[a] VSSI for Vatnaöldur eruption given as sum of eVolv2k VSSI for events in 876, 879 and 880 CE.

[b] Temperature anomalies for 822 not calculated due to potential interference from 817 CE eruption.

[c] Icelandic effusive eruption source for 817 CE Greenland volcanic sulfate suspected based on long duration volcanic sulfate flux [9]

Supplementary Table 3: Northern Hemisphere 3-year-mean summer temperature anomalies following tropical eruptions. Post-eruption 3-year mean temperature anomalies from the N-TREND[2], STO15[3] and SCH15[4] tree ring-based NH temperature reconstructions are listed, as well as the mean of all three reconstructions, and the ratio of the mean response to the estimated volcanic stratospheric sulfur injection (VSSI)[1].

Year	VSSI (Tg S)	$\Delta T_{3yr}^{N-TREND}$ (°C)	ΔT_{3yr}^{STO15} (°C)	ΔT_{3yr}^{SCH15} (°C)	ΔT_{3yr}^{ALL} (°C)	$\Delta T_{3yr}^{ALL}/VSSI$ (°C [Tg S]$^{-1}$)
1257	59.42	-0.64	-1.15	-0.54	-0.78	-0.01
1229	23.78	-0.41	-0.40	-0.35	-0.39	-0.02
1809	19.26	-0.42	-0.59	-0.22	-0.41	-0.02
1107	19.16	-0.43	-0.89	-0.47	-0.60	-0.03
1640	18.68	-0.99	-0.73	-0.55	-0.76	-0.04
1170	18.05	-0.55	-0.76	-0.39	-0.57	-0.03
1343	15.11	-0.32	-0.49	-0.30	-0.37	-0.02
1831	12.98	-0.33	-0.63	-0.34	-0.43	-0.03
1275	11.53	-0.14	-0.36	-0.13	-0.21	-0.02
1452	9.97	-0.74	-0.83	-0.37	-0.65	-0.06
1883	9.34	-0.25	-0.57	-0.46	-0.43	-0.05
1594	8.87	-0.04	-0.05	0.05	-0.01	0.00
1586	8.51	-0.29	-0.04	-0.27	-0.20	-0.02
1991	8.50	-0.02	0.24	0.12	0.11	0.01
1029	7.78	-0.34	-0.46	-0.10	-0.30	-0.04
973	6.24	0.01	-0.20	-0.08	-0.09	-0.01
916	6.08	0.17	-0.13	-0.08	-0.01	0.00
899	5.56	-0.53	-0.69	-0.04	-0.42	-0.08
1001	4.98	-0.05	-0.44	-0.25	-0.24	-0.05
1762	4.82	0.07	-0.25	-0.03	-0.07	-0.01
765	4.77	0.13	0.14	-0.02	0.08	0.02
1861	4.53	0.01	-0.16	-0.04	-0.06	-0.01
928	4.06	-0.01	0.00	-0.18	-0.06	-0.02
1963	3.90	-0.14	-0.13	-0.10	-0.13	-0.03
1982	3.75	0.08	0.33	-0.08	0.11	0.03
1653	3.70	0.21	0.08	-0.15	0.05	0.01
1125	3.68	-0.12	-0.06	-0.08	-0.09	-0.02
1388	3.26	-0.08	-0.55	-0.22	-0.28	-0.09
1902	3.20	-0.10	-0.23	-0.11	-0.15	-0.05
1553	2.41	-0.19	-0.24	0.02	-0.13	-0.06

Supplementary Table 4: Northern Hemisphere 3-year-mean summer temperature anomalies following explosive extratropical eruptions. Post-eruption 3-year mean temperature anomalies from the N-TREND[2], STO15[3] and SCH15[4] tree ring-based NH temperature reconstructions are listed, as well as the mean of all three reconstructions, and the ratio of the mean response to the estimated volcanic stratospheric sulfur injection (VSSI)[1].

Year	VSSI (Tg S)	$\Delta T_{3yr}^{N-TREND}$ (°C)	ΔT_{3yr}^{STO15} (°C)	ΔT_{3yr}^{SCH15} (°C)	ΔT_{3yr}^{ALL} (°C)	$\Delta T_{3yr}^{ALL}/VSSI$ (°C [Tg S]$^{-1}$)
1180	10.05	-0.31	-0.28	-0.20	-0.26	-0.03
1730	4.82	-0.20	-0.74	-0.33	-0.42	-0.09
1912	3.69	-0.26	-0.45	-0.25	-0.32	-0.09
1328	3.69	-0.32	-0.58	-0.19	-0.36	-0.10
1667	3.48	-0.19	-0.42	-0.06	-0.22	-0.06
1739	3.44	-0.12	-0.59	-0.09	-0.27	-0.08
1212	3.29	-0.08	0.09	0.08	0.03	0.01
1201	3.29	-0.04	-0.08	-0.13	-0.08	-0.02
1567	2.51	-0.39	-0.10	-0.32	-0.27	-0.11
798	2.48	-0.40	-0.60	-0.48	-0.49	-0.20
853	2.48	-0.61	-0.44	-0.33	-0.46	-0.18
1508	2.30	-0.13	-0.03	0.03	-0.04	-0.02

Supplementary Table 5: Northern Hemisphere 3-year-mean summer temperature anomalies following explosive extratropical eruptions before 750 CE. Post-eruption 3-year mean temperature anomalies from the N-TREND[2], STO15[3] and SCH15[4] tree ring-based NH temperature reconstructions are listed, as well as the mean of all three reconstructions, and the ratio of the mean response to the estimated volcanic stratospheric sulfur injection (VSSI)[1].

Year	VSSI (Tg S)	$\Delta T_{3yr}^{N\text{-}TREND}$ (°C)	ΔT_{3yr}^{STO15} (°C)	ΔT_{3yr}^{SCH15} (°C)	ΔT_{3yr}^{ALL} (°C)	$\Delta T_{3yr}^{ALL}/VSSI$ (°C [Tg S]$^{-1}$)
536	18.81	NA	-1.35	NA	-1.35	-0.07
626	13.20	NA	-0.38	-0.33	-0.35	-0.03

Supplementary Table 6: MAECHAM5-HAM ensemble simulation overview.

Eruption location	Volcano, country	Injection height	Ensemble size (eruption month)
4°S, 152°E	Rabaul, Papua New Guinea	30 hPa (23 km)	5 January +5 July
15°N, 91°W	Atitlan, Guatemala	30 hPa (23 km)	5 January +5 July
36°N, 138°E	Haruna, Japan	30 hPa (23 km)	5 January +5 July
56°N, 158°W	Aniakchak, USA	30 hPa (23 km)	5 January +5 July
56°N, 158°W	Aniakchak, USA	100 hPa (16 km)	5 January +5 July
56°N, 158°W	Aniakchak, USA	150 hPa (13 km)	5 January +5 July

Supplementary Table 7: Estimated years of tropical and extratropical eruptions common to the eVolv2k[1], Gao et al. (2008)[10] and Crowley and Unterman (2013)[11] volcanic reconstructions.

Category	eVolv2k year	Gao et al. (2007) year	Crowley and Unterman (2013) year
Tropical	1991	1991	1991
Tropical	1982	1982	1982
Tropical	1963	1963	1963
Tropical	1883	1883	1883
Tropical	1809	1809	1809
Tropical	1762	1761	1762
Tropical	1452	1452	1451
Tropical	1257	1258	1257
Extratropical	1912	1912	1912
Extratropical	1730	1729	1731

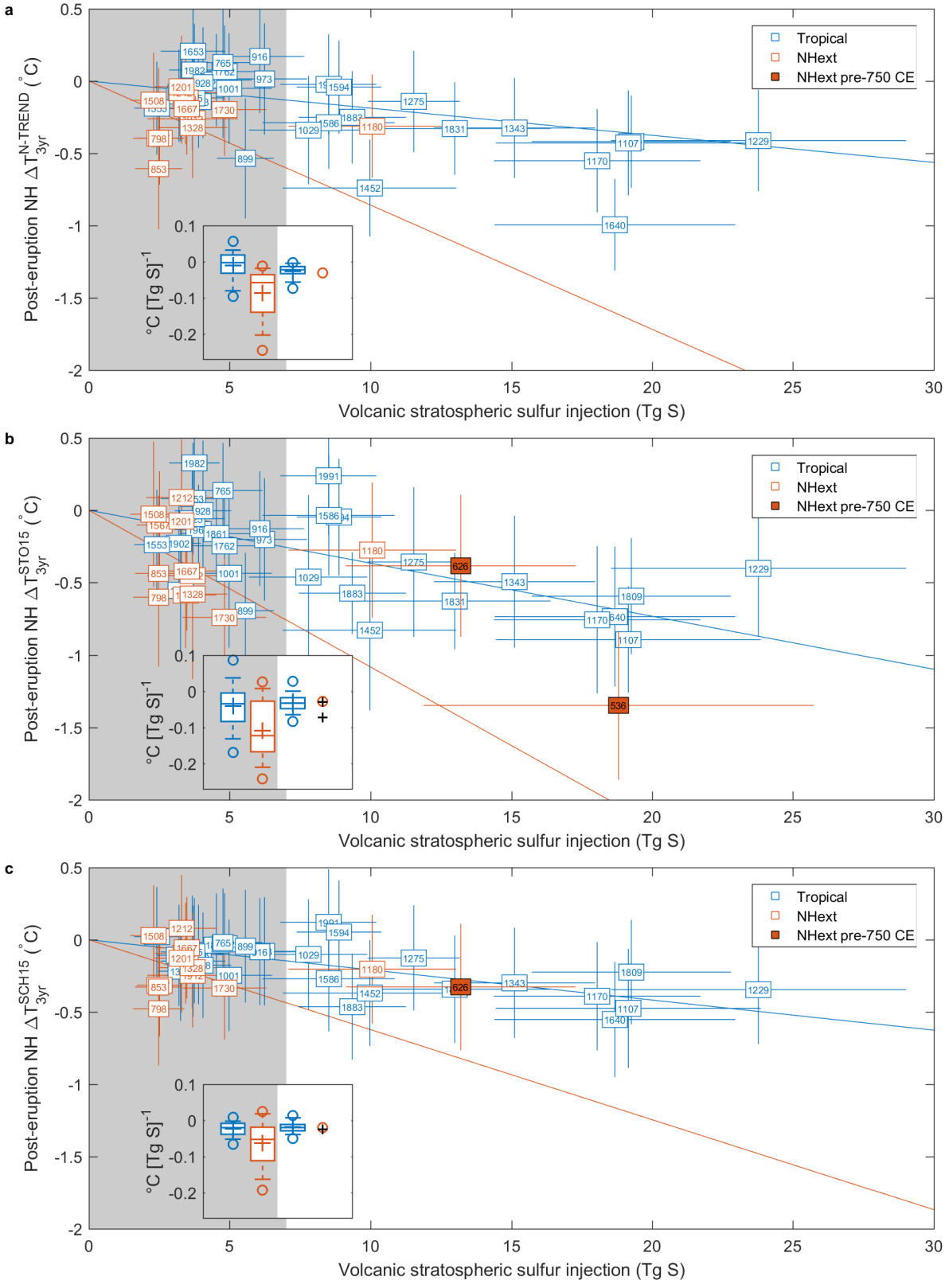
a
b
c
Tropical
NHext
NHext pre-750 CE
Post-eruption NH ΔT3yr N-TREND (°C)
Post-eruption NH ΔT3yr STO15 (°C)
Post-eruption NH ΔT3yr SCH15 (°C)
°C [Tg S]-1
Volcanic stratospheric sulfur injection (Tg S)

Supplementary Figure 1: Post-volcanic Northern Hemisphere temperature response to NH extratropical and tropical eruptions in relation to volcanic stratospheric sulfur injection in three tree ring-based reconstructions. Three-year mean temperature anomalies from the (**a**) N-TREND[2] and (**b**) STO2015[3] and (**c**) SCH2015[4] reconstructions are plotted as a function of the estimated volcanic stratospheric sulfur injection (VSSI, Tg [S]) for (blue) tropical and (orange) extratropical explosive eruptions. Numbers in the boxes indicate eruption years. Vertical and horizontal error bars represent ±1σ uncertainties. The 1257 Samalas eruption with VSSI=59.4 Tg S (Supplementary Table 4) lies outside the chosen limits of the plot. Temperature anomalies for NH extratropical events before 750 CE, which are based on a subset of the three reconstructions, are shown with orange-filled markers. Inset panels show boxplots of the distribution of three-year mean NH temperature anomalies per unit VSSI for each temperature reconstruction from (blue) tropical and (orange) extratropical explosive eruptions. Boxplots are shown separately for eruptions with VSSI less than 7 Tg S (gray shading on both plots) and the eruptions with VSSI greater than 7 Tg S. In each box, crosses denote the distribution mean, horizontal line the median, box the 25-75% interquantile range, whiskers the 1-99% interquantile range, and outliers are marked with circles. For the small sample of extratropical eruptions with VSSI>7 Tg, markers show cooling-to-VSSI ratios for individual eruptions: eruptions after 750 in orange, and pre-750 eruptions in black. For illustration, lines with slopes of the mean cooling-to-VSSI ratio for both tropical and extratropical are shown on the main panel.

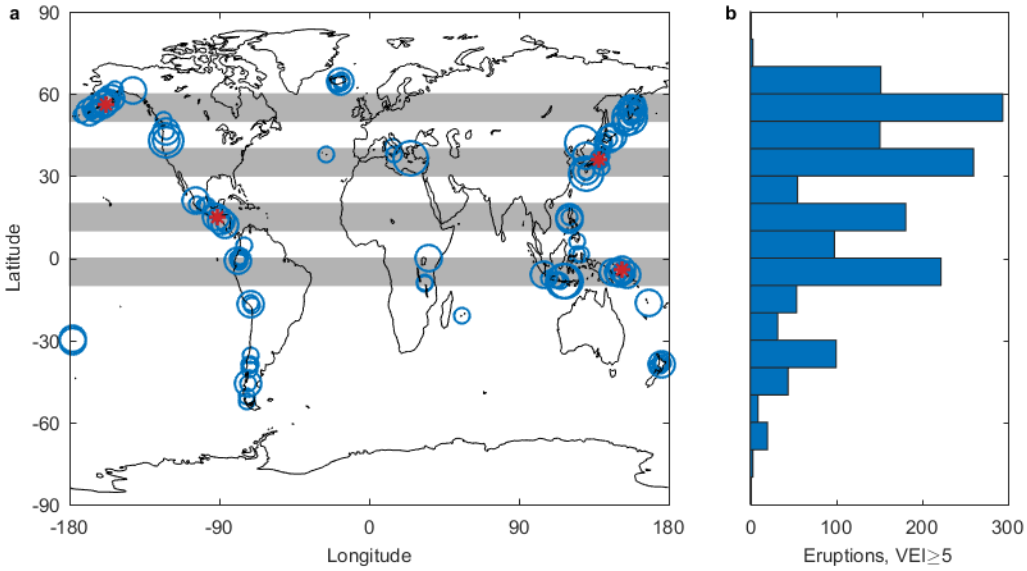

Supplementary Figure 2: Geographical distribution of identified Holocene (10,000 ka BP to present) eruptions with volcanic explosivity index[12] (VEI) ≥ 5 from the Volcanoes of the World database[13]. (left) World map with locations of identified VEI ≥ 5 eruptions marked by blue circles. (right) Histogram of eruption latitudes, binned into 10° latitude bins. The four latitude bands with largest eruption counts, accounting for 57% of the total, are shaded gray on the global map. Locations of the eruptions specified in MAECHAM5-HAM simulation ensembles shown by red markers.

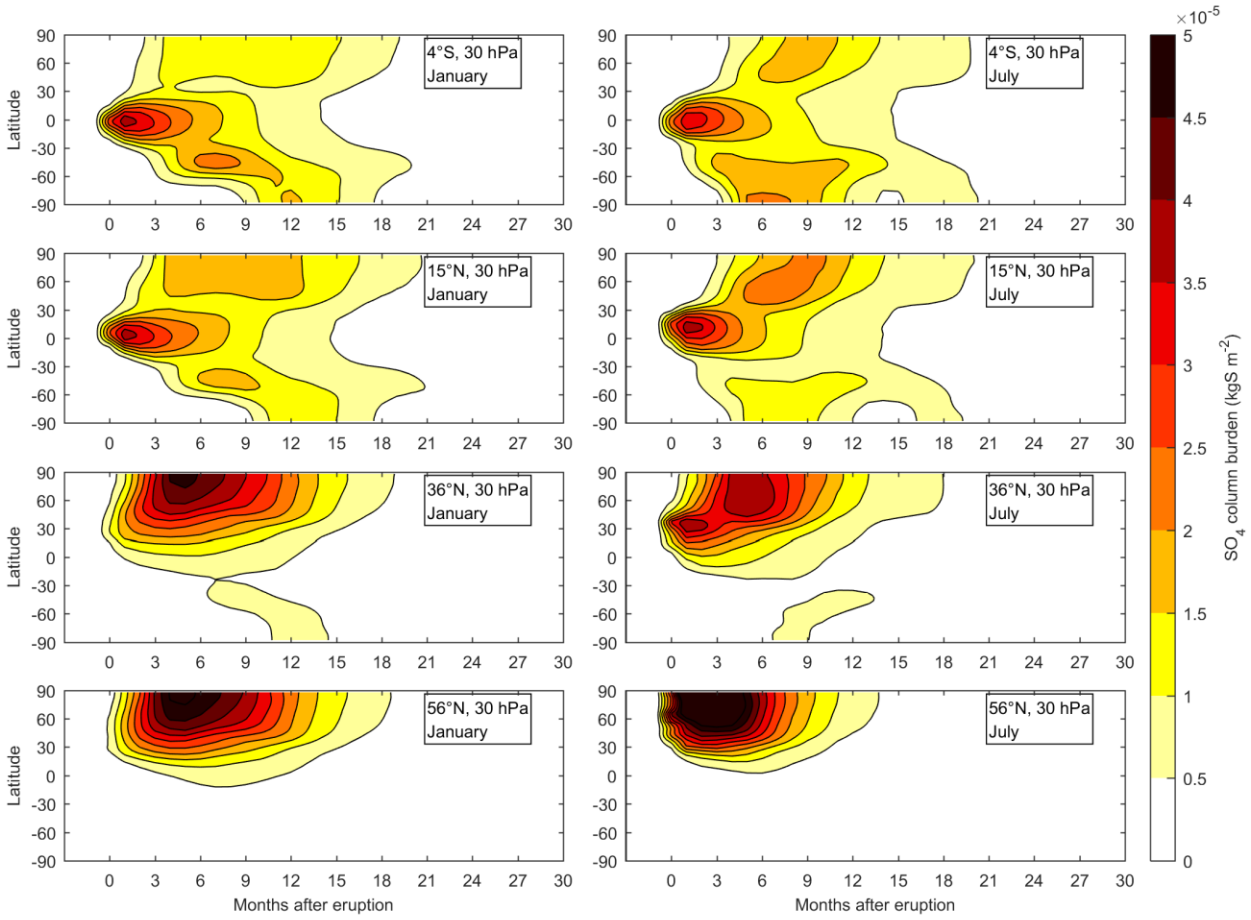

Supplementary Figure 3: MAECHAM5-HAM simulated ensemble mean zonal mean sulfate burden time series. Results are shown for eruptions simulations with injection at 30 hPa for January (left) and July (right), with eruption latitudes as labeled.

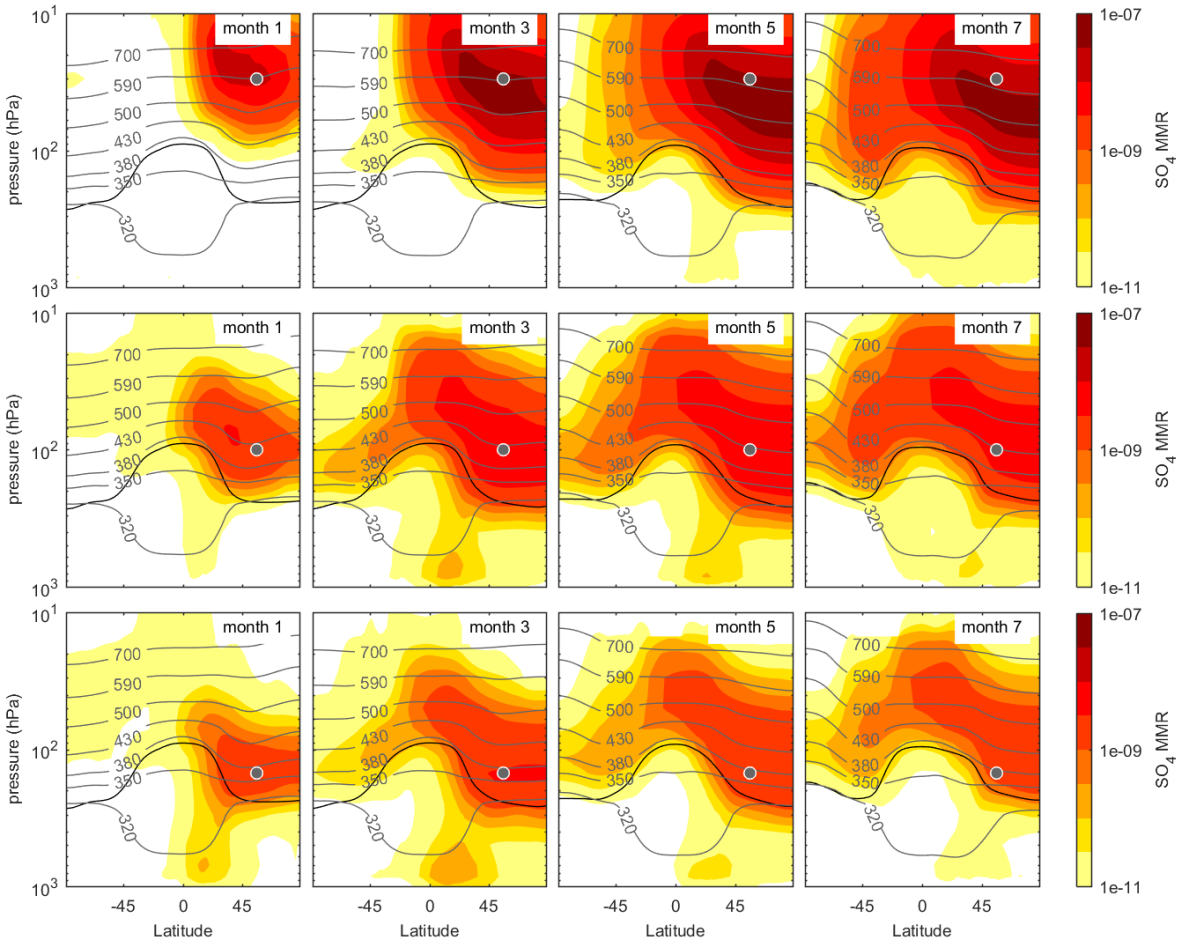

Supplementary Figure 4: Simulated ensemble mean, zonal mean volcanic sulfate mass-mixing ratio for January extratropical eruptions with varying injection heights. Sulfate mass-mixing ratio (SO_4 MMR) is shown for simulations with sulfur injections at 56°N and (top) 30 hPa, (middle) 100 hPa and (bottom) 150 hPa, for months 1, 3, 5, and 7 after the eruption, as labeled. Stratospheric sulfur injection locations are marked by gray markers in all panels. The climatological tropopause is marked by the black line, and surfaces of constant potential temperature are marked by gray contours.

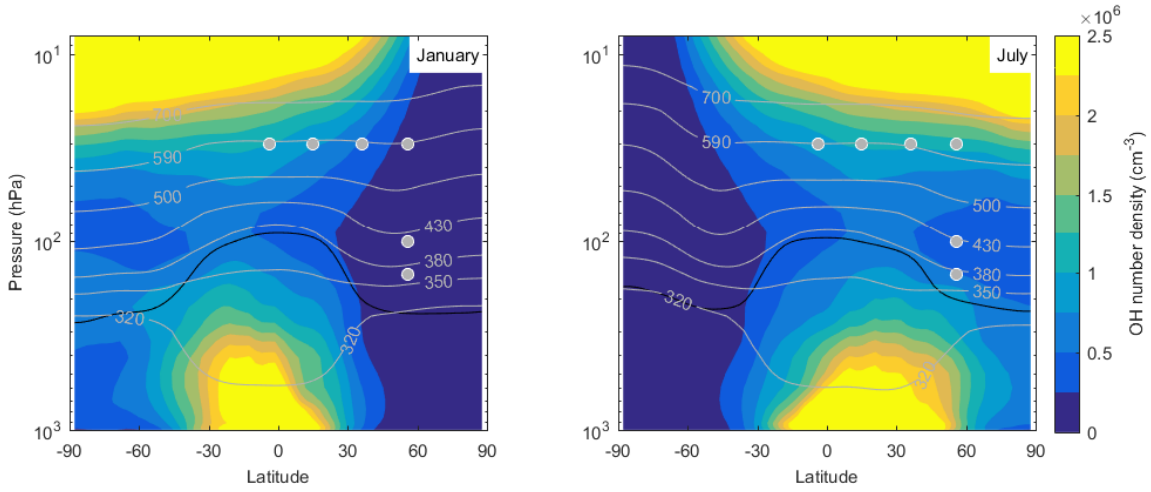

Supplementary Figure 5: Zonal mean OH number density in January and July, prescribed in the MAECHAM5-HAM simulations. Locations of SO_2 injection for the simulations are marked with gray markers. The climatological tropopause is marked by the black line, and surfaces of constant potential temperature are marked by gray contours.

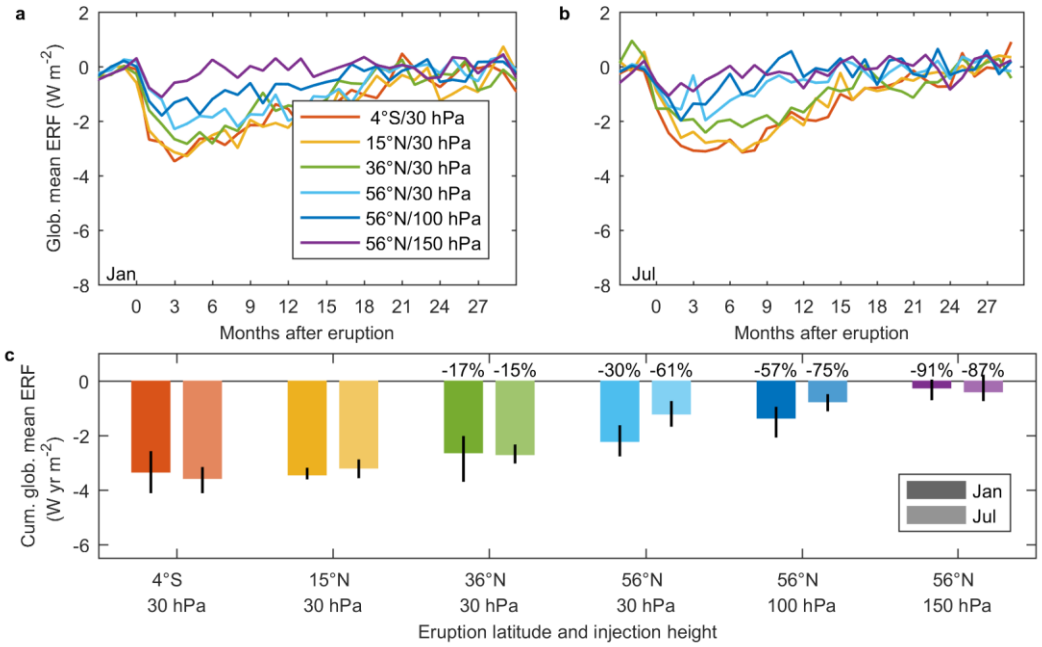

Supplementary Figure 6: Simulated global mean volcanic effective radiative forcing. Shown are (a,b) effective radiative forcing (ERF) for simulated eruptions of 8.5 Tg S in (left) January and (right) July. Line colors denote injection latitude and heights as listed in legend of panel (a). Three-year cumulative global mean ERF is shown in panel (c) as a function of injection latitude and height. For the extratropical injection cases, text labels show the percent difference of cumulative ERF with respect to the mean of the tropical (4°S and 15°N, 30 hPa) injection eruption simulations.

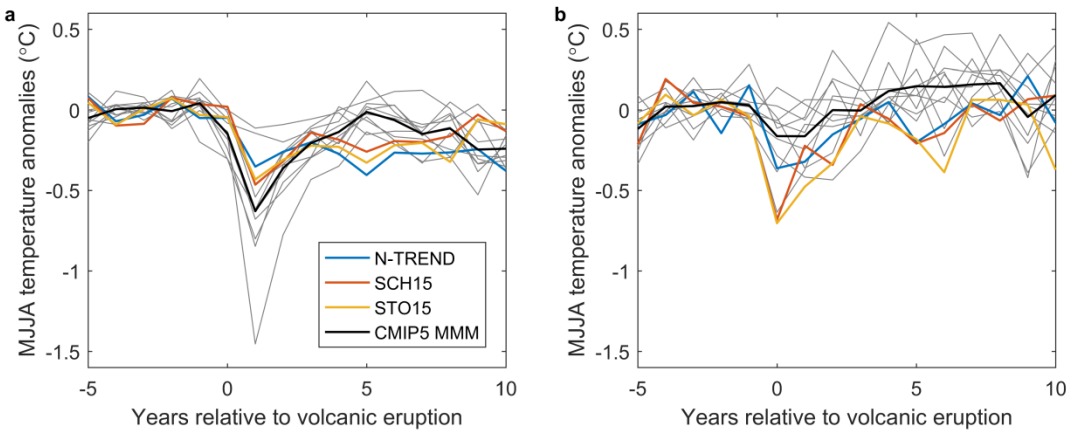

Supplementary Figure 7: Tree ring NH summer temperature and CMIP5/PMIP3 model mean response to major (a) tropical and (b) extratropical explosive volcanic eruptions. Only volcanic events common to the eVolv2k[1], Gao et al. (2008)[10] and Crowley and Unterman (2013)[11] volcanic forcing reconstructions in the period 750-2000 CE are used here: volcanic events are extracted from the model simulations depending on the volcanic forcing used, as given in Supplementary Table 7. CMIP5/PMIP3 models are those used in Ref [2]. Volcanic composites for individual CMIP5/PMIP3 model simulations are shown in gray, and the multi-model mean in black. Model temperatures represent 45-90°N area-weighted averages for May-August.

References

1. Toohey, M. & Sigl, M. Volcanic stratospheric sulfur injections and aerosol optical depth from 500 BCE to 1900 CE. *Earth Syst. Sci. Data* **9,** 809–831 (2017).

2. Wilson, R. *et al.* Last millennium northern hemisphere summer temperatures from tree rings: Part I: The long term context. *Quat. Sci. Rev.* **134,** 1–18 (2016).

3. Stoffel, M. *et al.* Estimates of volcanic-induced cooling in the Northern Hemisphere over the past 1,500 years. *Nat. Geosci.* **8,** 784–788 (2015).

4. Schneider, L. *et al.* Revising midlatitude summer temperatures back to A.D. 600 based on a wood density network. *Geophys. Res. Lett.* **42,** 4556–4562 (2015).

5. Thordarson, T. & Larsen, G. Volcanism in Iceland in historical time: Volcano types, eruption styles and eruptive history. *J. Geodyn.* **43,** 118–152 (2007).

6. Oppenheimer, C. *et al.* The Eldgjá eruption: timing, long-range impacts and influence on the Christianisation of Iceland. *Clim. Change* **147,** 369–381 (2018).

7. Schmid, M. M. E., Dugmore, A. J., Vésteinsson, O. & Newton, A. J. Tephra isochrons and chronologies of colonisation. *Quat. Geochronol.* **40,** 56–66 (2017).

8. Büntgen, U. *et al.* Multi-proxy dating of Iceland's major pre-settlement Katla eruption to 822–823 CE. *Geology* **45,** 783–786 (2017).

9. Sigl, M. *et al.* A new bipolar ice core record of volcanism from WAIS Divide and NEEM and implications for climate forcing of the last 2000 years. *J. Geophys. Res. Atmos.* **118,** 1151–

1169 (2013).

10. Gao, C., Robock, A. & Ammann, C. Volcanic forcing of climate over the past 1500 years: An improved ice core-based index for climate models. *J. Geophys. Res.* **113,** D23111 (2008).

11. Crowley, T. J. & Unterman, M. B. Technical details concerning development of a 1200 yr proxy index for global volcanism. *Earth Syst. Sci. Data* **5,** 187–197 (2013).

12. Newhall, C. G. & Self, S. The volcanic explosivity index (VEI) an estimate of explosive magnitude for historical volcanism. *J. Geophys. Res.* **87,** 1231 (1982).

13. Global Volcanism Program. in *Smithsonian Institution* (ed. Venzke, E.) (2013).